ACS Chemical Neuroscience

Article

Novel isatin thiosemicarbazone derivatives as potent inhibitors of #-amyloid peptide (##) aggregation and toxicity

Marina Sagnou, Barbara Mavroidi, Archontia Kaminari, Nikos Boukos, and Maria Pelecanou

ACS Chem. Neurosci., **Just Accepted Manuscript** • DOI: 10.1021/acschemneuro.0c00208 • Publication Date (Web): 29 Jun 2020

is published by the American Chemical Society. 1155 Sixteenth Street N.W., Washington, DC 20036

Novel isatin thiosemicarbazone derivatives as potent inhibitors of *β*-amyloid peptide (A*β*) aggregation and toxicity

Marina Sagnou[1*], Barbara Mavroidi[1], Archontia Kaminari[1], Nikos Boukos[2], Maria Pelecanou[1]

[1]Institute of Biosciences & Applications, National Centre for Scientific Research "Demokritos", 15310 Athens, Greece

[2]Institute of Nanoscience and Nanotechnology, National Centre for Scientific Research "Demokritos", 15310 Athens, Greece

Corresponding Author

[*] Marina Sagnou, Institute of Biosciences &Applications, National Centre for Scientific Research "Demokritos", Patriarhou Grigoriou & Neapoleos 27, 15310, Athens, Greece; E-mail: sagnou@bio.demokritos.gr

ABSTRACT

Inhibition of the amyloid *β*-peptide (A*β*) aggregation of Alzheimer's disease (AD) is among the therapeutic approaches against AD which still attracts scientific research interest. In the search for compounds that interact with A*β* and disrupt its typical aggregation course towards oligomeric or polymeric toxic assemblies, small organic molecules of natural origin, combining low molecular weight (necessary blood-brain barrier penetration) and low toxicity (necessary for pharmacological application), are greatly sought after. Isatin (1H-indoline-2,3-dione), a natural endogenous indole, and many of its derivatives exhibit a wide spectrum of neuropharmacological and chemotherapeutic properties. The synthesis and biological evaluation of four new isatins as inhibitors of A*β* aggregation is presented herein. In these derivatives the N-phenyl thiosemicarbazide moiety is joined at the 3-oxo position of isatin through Schiff base formation, and substitutions are present at the indole nitrogen and position 5 of the isatin core. Biophysical studies employing circular dichroism, thioflavin T fluorescence assay and transmission electron microscopy reveal the potential of the ITSCs to alter the course of A*β* aggregation, with two of the derivatives exhibiting outstanding inhibition of the aggregation process, preventing completely the formation of amyloid fibrils. Furthermore, in *in vitro* studies in primary neuronal cell cultures, the ITSCs were found to inhibit the A*β*-induced neurotoxicity and reactive oxygen species (ROS) production, at concentrations as low as 1 μM. Taken all together, the novel ITSCs can be considered as privileged structures for further development as potential AD therapeutics.

Keywords:

Alzheimer's disease; *β*-Amyloid peptide; Isatin thiosemicarbazones; Inhibitors of *β*-amyloid aggregation, Circular dichroism spectropolarimetry; Primary neuronal cell cultures; Antioxidant activity

INTRODUCTION

Isatin (1H-indole-2,3-dione) (**1**, Figure 1) is a well-known natural product which can be found in plants of *Genus Isatis* and *Couroupita Guianensis*. This indolic derivative is known in the chemical industry for nearly 140 years, as it is a product of indigo dye oxidation by means of nitric and chromic acid.[1-5] It is an endogenous oxidized indole present in the mammalian brain, peripheral tissues and body fluids[6], originally identified in humans as one component of the monoamine oxidase inhibitory activity.[7] Isatin has been extensively studied in behavioral and metabolic assays and >90 proteins have been identified through proteomic analysis as its potential biological targets .[8] It acts as a potent inhibitor of human mitochondrial monoamine oxidase B (MAO-B)[9] and administered exogenously was found to significantly increase the levels of acetylcholine, choline and dopamine in rat brain tissues.[10] It is a flexible and versatile synthetic scaffold, consisting of an indole nucleus and two types of carbonyl groups, a keto and a lactam group that render it a favorable building block for Schiff base reactions, heterocyclic compound synthetic strategies and pharmacophore development.[11]

Isatin derivatives possess a wide range of biological activities, including antimicrobial, anti-HIV, antiviral, antimalarial, anticancer, anticonvulsant, anti-asthmatic, antiinflammatory and analgesic activities.[12,13] Isatin derivatives have also been studied as potential therapeutic agents against Alzheimer's disease (AD).[14-20] More specifically, a library of N-substituted isatin 3-benzoylhydrazones has been explored as β-secretase (BACE-1) inhibitors using a virtual high-throughput screening (HTS) approach.[14] Furthermore, out of eight compounds sorted out in a HTS based on the fluorescence of Aβ42-GFP fusions on a collection of 65,000 small molecules, compound D737 (**2**, Figure

1), a 2-oxoindole derivative, proved to be the most effective in inhibiting Aβ42 aggregation, reducing Aβ42-induced toxicity in neuronal cells, as well as increasing the life span and locomotive ability of flies in a Drosophila melanogaster model of AD.[15] Campagna, Catto and their colleagues have extensively studied a series of isatin-3-arylhydrazones[16] (**3**, Figure 1) and other related molecules as inhibitors of Aβ40 aggregation revealing interesting structure activity relationships like [17-20] the role of lipophilicity, the positive contribution of the 5-methoxy substitution on the isatin core and the opportunity of alkylating the indole nitrogen for efficient aggregation inhibition.[16]

The findings are in agreement with the general notion that indole derivatives interact with Aβ, blocking its self-assembly and fibril formation, by interfering with π–π interactions or π-stacking, hydrophobic forces and electrostatic interactions between the Aβ side chains and/or by effectively forming polar interactions and/or hydrogen bond with Aβ moieties.[21-23]

Based on the encouraging results of isatin-3-arylhydrazones and in view of our ongoing investigation on isatin-3-thiosemicarbazones (ITSCs)[24,25] and AD therapeutics[26,27] we report herein the synthesis and biological evaluation of four novel ITSCs as inhibitors of Aβ aggregation and neuronal cell toxicity. The thiosemicarbazone (TSC) moiety has been utilized in the synthesis of metal complexes able to interfere with Aβ peptide aggregation or up-regulate Aβ peptide degrading enzymes. More specifically, copper-bis(thiosemicarbazonato) and Ru(II)-p-cymene thiosemicarbazone complexes have shown interesting biological activities as potential Aβ aggregation inhibitors.[28,29] Furthermore, recent work by Kulkarni and his colleagues showed that a 3-acetylcoumarin thiosemicarbazone profoundly inhibits the formation of higher aggregates of Aβ peptide

compared to acetylcoumarin alone.[30,31] Also, the TSC moiety provided additional benefit to the acetylcoumarin molecule in rescuing Aβ42 induced toxicity in neuronal SH-SY5Y cells and reduced its cell toxicity, whereas results from docking studies showed that the thiosemicarbazone moiety plays an important role due to its capacity for formation of hydrogen bonding contacts with peptide residues. Therefore, it was reasonable to anticipate that the combination of the thiosemicarbazone moiety with the isatin core may generate active agents with anti-amyloid activity. The four new compounds were evaluated in detail with circular dichroism (CD), thioflavin T (ThT) fluorescence assay, and transmission electron microscopy (TEM), for their potential to inhibit the assembly of Aβ into oligomeric/polymeric aggregates and the eventual formation of amyloid fibrils. Furthermore, the effect of the ITSCs on the cytotoxic and ROS producing activity of Aβ was evaluated in primary neuronal cells.

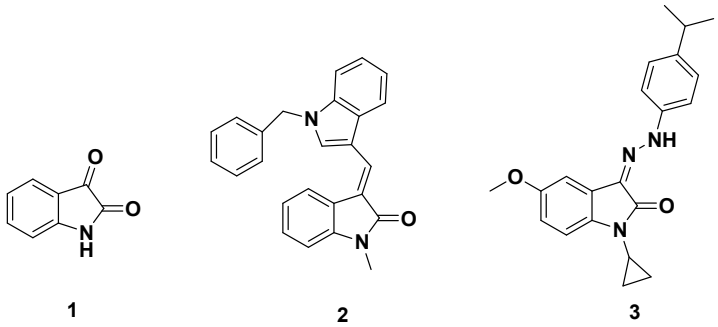

Figure 1. Chemical structures of isatin (**1**) and other active indole derivatives (**2**, **3**) in the literature.

RESULTS AND DISCUSSION

Design. A preliminary screening of 13 structurally related ITSCs (see Supporting Information) for their potential to inhibit aggregation of Aβ40 was conducted by means of CD. The structures were designed aiming to investigate the potential contribution of

the isatin substitution at position 5- and the *para*- substitution of the phenyl thiosemicarbazone moiety (Figure 2). Out of the 13 structurally related ITSCs only compounds **4** and **5** (Figure 3), when co-incubated with Aβ peptide, resulted in a considerable alterations of the characteristic CD spectrum of the Aβ peptide compared to spectrum of the peptide alone. The rest of the ITSCs did not affect the CD spectrum of the Aβ peptide at all, suggesting the lack of any interaction with the peptide.

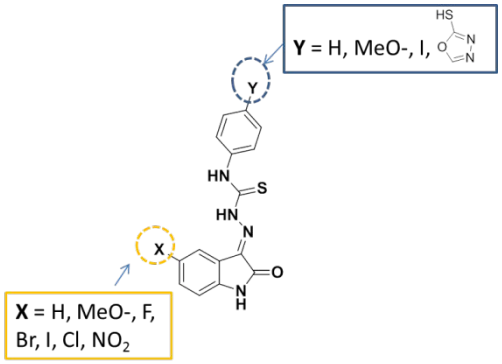

Figure 2. The design of the initial library of ITSCs

Consequently, ITSCs **4** and **5** were further converted to the piperidine N-Mannich base derivatives **6** and **7**, respectively (Figure 3). This was based on literature reports stating that Mannich base moieties exhibit good antioxidant,[32,33] anti-inflammatory[34] and AChE inhibitory[35] activities, rendering them useful in the anti-amyloid drug design.

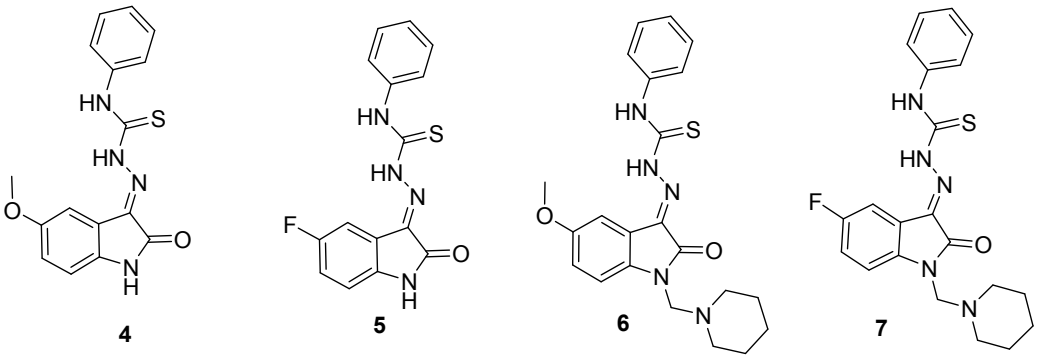

Figure 3. Chemical structures of the ITSC derivatives **4 - 7** of this work.

Synthesis. Compounds **4** and **5** were synthesized in high yield reactions between 5-methoxy- or 5-fluoroisatin, respectively, with phenyl thiosemicarbazide, using acetic acid as a catalyst to initiate the reaction, based on reported methods (Scheme 1).[36] In both cases the desired product precipitated out of the reaction mixture and was collected in pure form after a single recrystallization from ethanol. It is worth noting that this simple, high yielding, and low-cost preparation of scaffolds with pharmacophoric potential is a highly advantageous and desirable feature. The Mannich bases, **6** and **7**, were consequently prepared by condensing the acidic isatin NH-group of **4** and **5,** respectively, with formaldehyde and piperidine.[37] The Mannich reactions were of equally high yield as the preceding Schiff reactions (Scheme 1).

All compounds were characterized by ^{1}H and ^{13}C NMR spectroscopy as well as MS-ESI (Supporting Information). The ITSC derivatives are soluble in $CHCl_3$, DMSO, DMF and they are stable in organic solvents for at least a month as witnessed by NMR.

Scheme 1. Synthetic route of the ITSC derivatives[a]

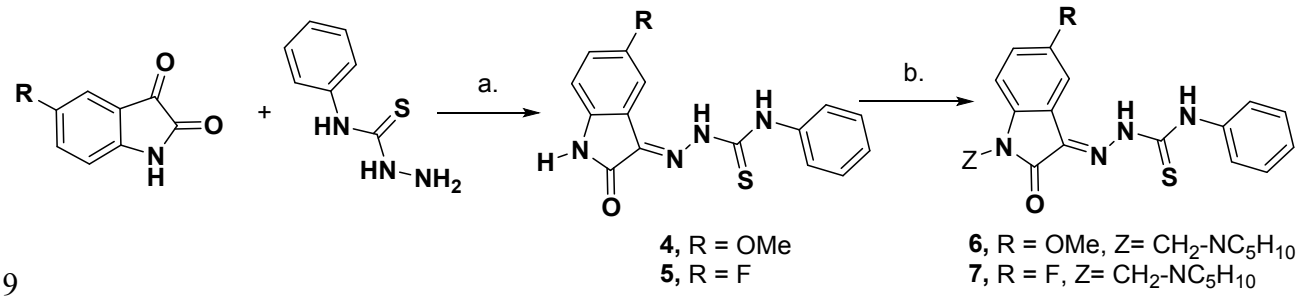

[a]Reagents and conditions: (a) ethanol, cat. CH_3COOH, Reflux; (b) formaldehyde, piperidine.

CD studies of the inhibition of A*β*40 and A*β*42 aggregation. Circular dichroism (CD) spectropolarimetry was employed to assess the effect of the ITSCs on the aggregation process of A*β*40 and A*β*42 during a 30-day course. As can be seen in Figure 3 for the A*β*40 (top left) and A*β*42 (top right) peptides, the typical aggregation process of A*β* produces characteristic CD spectra over time reflecting the conformational changes that take place in solution: the random coil A*β* monomers are gradually converted into *β*-sheet assemblies, finally producing insoluble amyloid fibrils that precipitate from solution with loss of CD signal. [38]

It is evident from the spectra in Figure 4 (left column) that the addition of compounds **4** and **7** in solutions of A*β*40 at a ratio of 1:1 strongly inhibited its aggregation. The CD spectra essentially remained at random coil conformation (min at 198 nm) with a small reduction in intensity as time proceeded and without any further transformation, even at day 30. In the presence of derivatives **5** and **6**, a decrease in the intensity of the random coil trace was observed, suggesting the formation of amyloid fibrils, though with considerable delay compared to solutions of plain A*β*40. More specifically, in the case of derivative **5**, a shift of the absorption minimum to higher wavelengths (200 nm) was noted and the signal approached zero at day 30, while in derivative **6** the random coil minimum at 198 nm remained stable and CD signal was still present at day 30. The interaction of compounds **4** and **7** with A*β*42, which is more fibrillogenic and aggregates faster than A*β*40,[39] was even more pronounced. Right from the beginning, composite peaks between random coil and *β*-sheet appeared, with minima at 205 and 217 nm that

remained unchanged in solution for the whole duration of the study with no sign of fibril formation. Corresponding experiments in the presence of compounds **5** and **6** revealed once again their effect to delay the typical Aβ aggregation process, though not preventing fibril formation leading to almost complete signal loss at day 30.

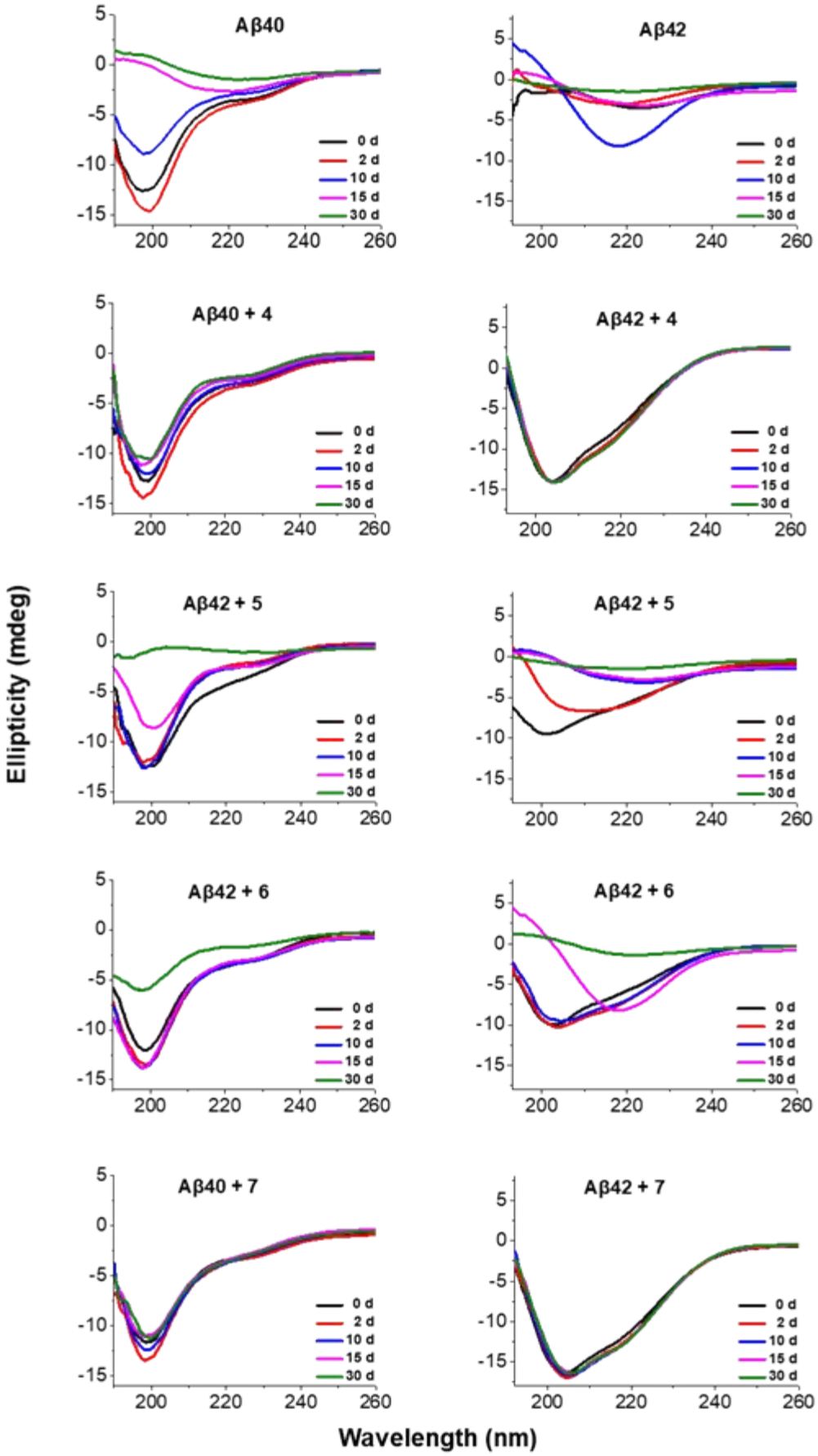
Aβ40
Aβ42
Aβ40 + 4
Aβ42 + 4
Aβ42 + 5
Aβ42 + 5
Aβ42 + 6
Aβ42 + 6
Aβ40 + 7
Aβ42 + 7
0 d
2 d
10 d
15 d
30 d
Ellipticity (mdeg)
Wavelength (nm)

Figure 4. CD spectra of plain solutions of Aβ40 and Aβ42 (50 μM) as well as in the presence of the ITSC derivatives (Aβ:ITSCs ratio 1:1). Spectra were recorded for a period of 30 days at 37 °C. Representative spectra from n = 3 independent experiments are presented.

ThT test for the detection of typical amyloid fibrils. The aged for 30 days solutions of the CD study were subsequently subjected to the thioflavin T (ThT) binding assay that detects amyloids fibrils. Specifically, the ThT dye, which is negligibly fluorescent in solution, displays significant fluorescence enhancement upon binding to typical amyloid fibrils.[40] As it is apparent in Figure 5 (black line) the ThT assay of plain solutions of Aβ40 and Aβ42 resulted in considerable fluorescence signal indicative of fibril formation. This fluorescence signal was dramatically decreased when either Aβ40 or Aβ42 were incubated with **4** or **7** for 30 days, a finding which indicates the lack of fibrils in solution, and is in agreement with the CD data. The presence of **5** and **6** in solutions of Aβ40 (Figure 5A) resulted in reduced fluorescence intensity, compared to plain Aβ40, indicating reduction in fibril formation. Furthermore, the shift in fluorescence maximum to higher wavelengths may suggest the presence of fibrils of differentiated structure compared to typical Aβ40 fibrils. The presence of compounds **5** and **6** in solutions of Aβ42 (Figure 5B) did not result in significant reduction of fluorescence intensity indicating that fibril formation remains almost unaffected. Again, the ThT results for compounds **5** and **6** are in complete agreement to the CD studies.

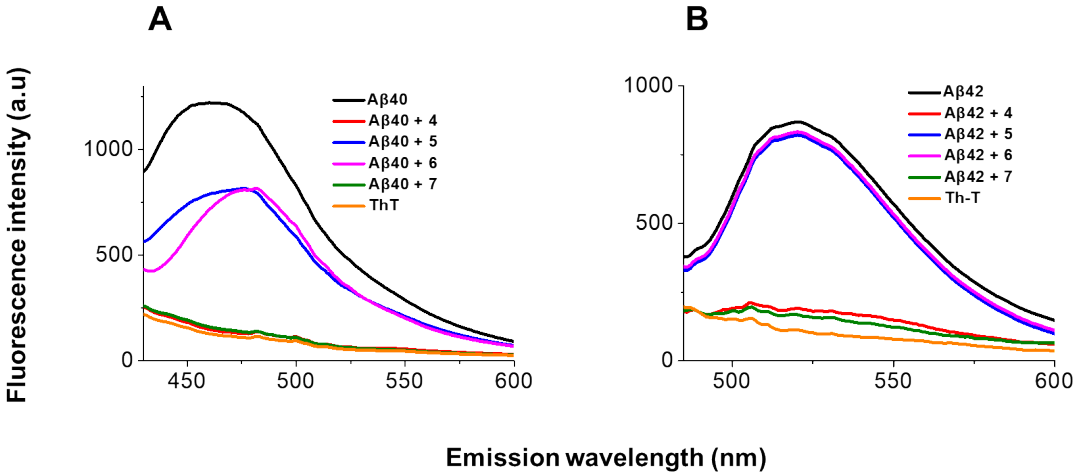

Figure 5. Aβ aggregation assay using fluorescence emission of ThT upon binding to aggregated Aβ (25 μM, 30 d). A lower intensity than that of plain Aβ solutions ThT (black line) indicates lower concentration of Aβ fibrils. (**A**) Aβ40 solutions in the absence and presence of ITSCs and (**B**) Aβ42 solutions in the absence and presence of ITSCs. Fluorescence was monitored after excitation at λ = 440 nm. Representative spectra from n = 3 independent experiments are presented.

TEM microscopy images of amyloid fibrils. To evaluate the effect of ITSCs on the occurrence and morphology of Aβ fibers, TEM microscopy was used employing the 30 day aged samples subjected to CD and ThT analysis. Images of plain Aβ42 solutions as well as after incubation with compounds **4** and **7** are presented in Figure 6. In the absence of any ITSCs the typical dense network of intertwined Aβ fibrils was observed.[41] However, upon incubation of Aβ with either **4** or **7**, the samples were devoid of fibrils and only a very small amount of sporadic crystal-like formations could be observed which may be attributed to a degree of self-organization of the ITSCs under the particular experimental conditions. The complete lack of fibrils is an impressive finding. To the best of our knowledge, it is the first time that a complete absence of Aβ typical fibrils or

other type of lower amorphous aggregates has been reported in the presence of an aggregation inhibitor. On the other hand, the corresponding aged Aβ42 samples containing **5** and **6,** displayed an extended fibrillar network, similar to the untreated control containing Aβ peptide alone (Figure 6). The results form TEM microscopy are in complete agreement with the CD and ThT findings providing further confirmation for the potential of **4** and **7** to effectively intervene in the Aβ40 and Aβ42 aggregation process and inhibit fibril formation.

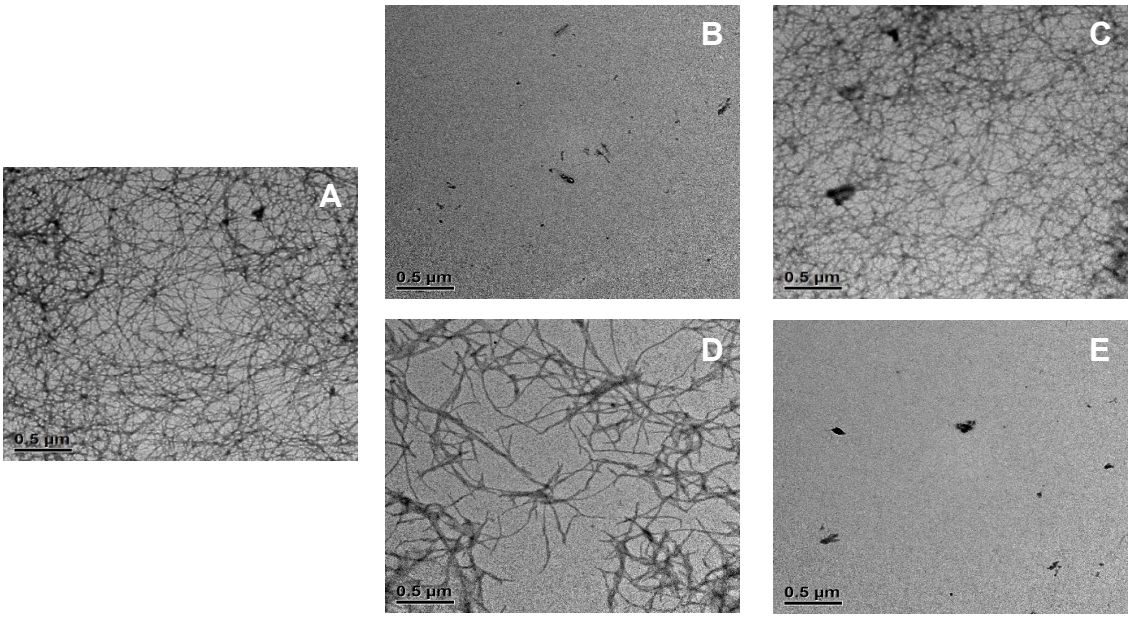

Figure 6. TEM images of the aged Aβ42 solutions (30 d, 50 µM) used for the CD evaluation in the absence (**A**) and the presence of compounds **4** and **7** (50 µM, **B** and **E**), where complete lack of fibrils was observed and **5** and **6** (50 µM, **C** and **D**) where fibril formation has taken place. The scale bars correspond to 0.5 µm. Representative images from n = 2 independent experiments are presented.

***In vitro* studies of inhibition of A*β* induced neurotoxicity.** A*β* is known to be cytotoxic in neuronal cells and inhibitors/modulators of its aggregation are often effective in reducing toxicity *in vitro* and *in vivo*.[42,43] To investigate whether the ITSCs can protect cells from A*β*-induced toxicity, the MTT cytotoxicity assay on primary mouse hippocampal cells was performed. Hippocampal neuronal cells are a suitable model for assessing A*β*-related toxicity since hippocampus plays a key role in learning and memory and is particularly vulnerable to damages at early stages of Alzheimer's disease.[44] Treatment of the primary neurons with A*β*40 (1 μM, Figure 7A) and A*β*42 (1 μM, Figure 7B) alone, resulted in a drop of cell viability to 63.4% and 52.5% compared to control (untreated cells). These viability measurements are in agreement with other literature findings which also report the enhanced neural cytotoxicity of A*β*42 relative to that of A*β*40.[45]The addition of ITSC derivatives in the culture medium resulted in inhibition of neurotoxicity of both A*β*40 and A*β*42 in a dose-dependent manner. More specifically, addition of **4** resulted in a considerable cell viability increase to 91.1% (A*β*40, 1:2 ratio) and 93.9% (A*β*42, 1:2 ratio). In a similar fashion, in the presence of **7**, cell survival was recovered to nearly control levels (89.9% for A*β*40 and 95% for A*β*42, 1:2 ratio). In the presence of **6** and **5** derivatives, the cell viability increase was lower, but still statistically significant, reaching 82.3% and 80.5% for A*β*40, 85.1% and 81% for A*β*42, respectively. The fact that all ITSCs were found to restrain A*β* induced neurotoxicity is in accordance with their potential to interact early on with A*β*, as revealed by the CD study. The stronger effect exhibited by **4** and **7** also correlates well with the stronger intervention of the compounds in A*β* aggregation, as revealed by the CD, ThT and TEM studies, and is in agreement with relevant studies.[15] Our results are in good agreement with literature

reports revealing the antiaggregation potential of the indole core, as exemplified by tabersonine[46] and melatonine.[47,48] However, tabersonine exhibited increased cytotoxicity and melatonine was used in much higher concentrations up to 50 μM to cause a comparable result.

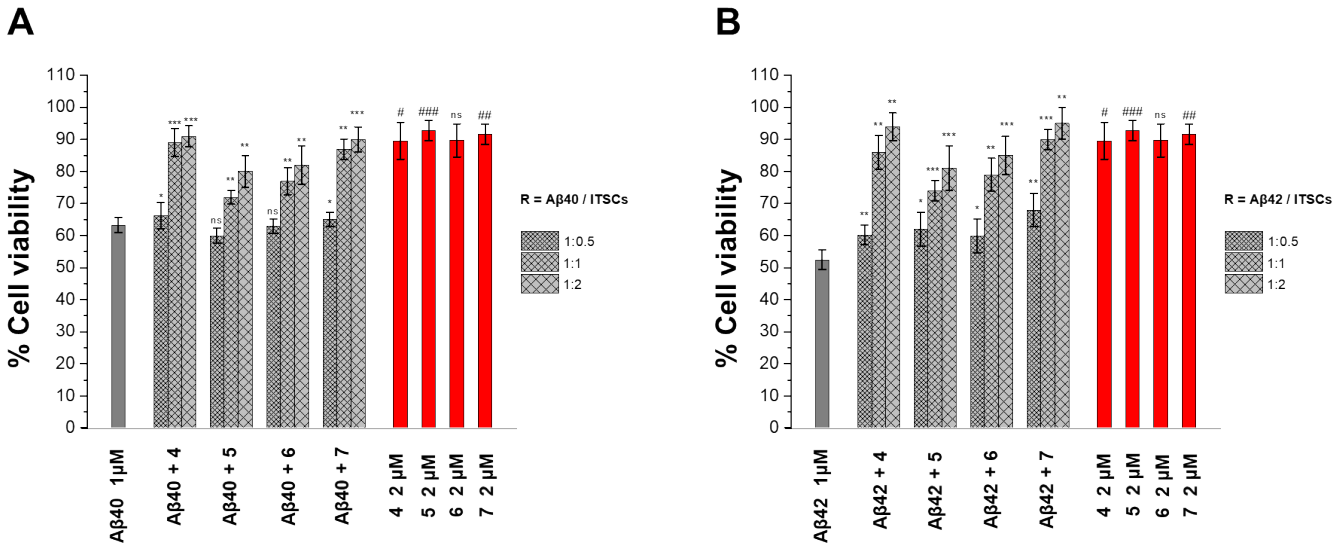

Figure 7. Effects of the ITSC derivatives (0.5, 1 and 2 μM) on the cytotoxicity of A*β*40 (**A**) or A*β*42 (**B**) (1 μM) in primary hippocampal neuronal cells after 24 h of incubation at 37 °C, as determined using the MTT assay (n = 3 independent experiments, each one performed in six replicates). The red bars represent the effect on the cell viability of ITSCs alone. The data are presented as mean ± SEM, $^{*}p \leq 0.05$, $^{**}p \leq 0.01$, $^{***}p \leq 0.001$, ns (not significant)>0.05 compared to A*β* (1 μM) treatment and $^{\#}p<0.01$ and $^{\#\#}p<0.01$, $^{\#\#\#}p<0.001$ compared to control (untreated cells).

In addition, qualitative assessment of the ITSC effect on cell viability and morphology of hippocampal primary cells exposed to A*β* was assessed by phase-contrast microscopy (Figure 8). A*β*-treated neurons (1 μM) demonstrated hallmarks of degeneration, such as

fragmented neurites, non-developed axons, cell shrinkage and membrane blebbings, that are in accordance with relevant literature data.[49] Addition of the ITSCs in the Aβ solutions in a 1:2 ratio alleviated the effects of Aβ toxicity and a substantial recovery of the Aβ-induced alterations was observed. In agreement to the MTT cytotoxicity data, the selected derivatives alone exerted no substantial alteration on the morphology of neuronal cells (data not shown). Both MTT results and microscopic examinations indicate that the ITSCs can effectively attenuate the cytotoxicity of Aβ in primary hippocampal cells.

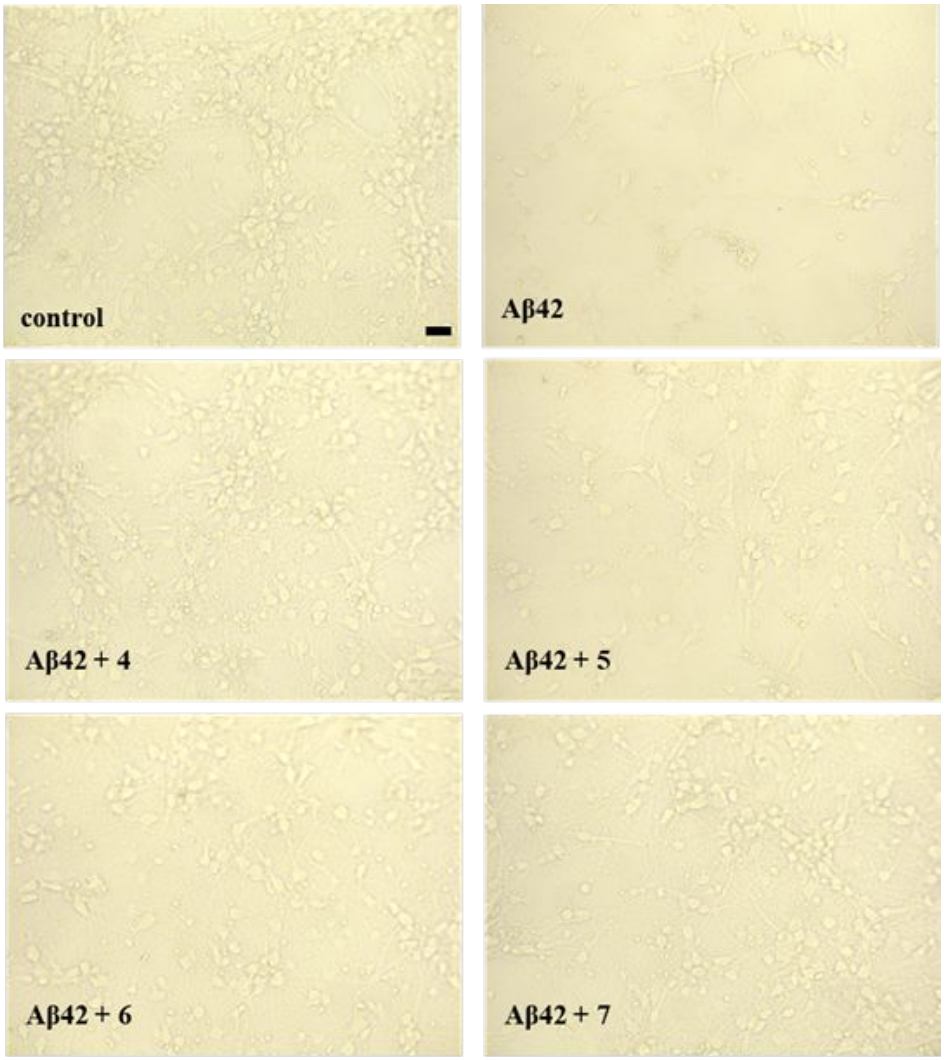

Figure 8. Phase-contrast microscopy images of primary hippocampal neuronal cells exposed for 24 h at 37 °C to pre-incubated A*β*42 solutions (1 μM) in the absence or in the presence of ITSC derivatives (2 μM). The scale bar corresponds to 50 μm. Representative images from n = 2 independent experiments are presented.

***In vitro* studies of inhibition of A*β* induced ROS production.** A*β* induced oxidative stress is linked to the pathogenesis and early development of AD. Elevated levels of A*β*

are associated with increased levels of oxidation products from proteins, lipids and nucleic acids in AD hippocampus and cortex[50,51]. Accumulated evidence suggests that ROS may be important mediators of A*β* neuronal cell death in the development of AD.[52] Hence, the effect of ITSCs on the levels of ROS generated by A*β* in hippocampal neuronal cells was evaluated by means of the DCFH-DA assay.[53] The results of the ROS assessment are summarized in Figure 9. Exposure of hippocampal cell cultures to A*β* solutions (1 μM) resulted in the production of considerable amount of ROS, as evidenced by the significant increase in DCF fluorescence.[54] Incubation of the cells with any of the four compounds **4 - 7** alone did not cause any significant change in the DCF fluorescence compared to untreated cells. On the contrary, as can be seen in Figure 9A for A*β*40, and 9B for A*β*42, co-incubation of the A*β* with **4** and **7** resulted in more than 50% reduction in DCF fluorescence indicating an important decrease in ROS production. Co-incubation of the A*β* solutions with derivatives **6** and **5** also resulted in lower intracellular ROS generation, but to a lesser extent. The studied ITSCs show the same trend in reducing ROS production and in protecting form A*β* cytotoxicity, with **4** and **7** showing the best results and **5** and **6** following in efficacy. Even though the mechanism of A*β* cytotoxicity and ROS production are still not clear,[55] our results provide a link between the potential of inhibitors to intervene in A*β* aggregation and to decrease ROS production that may add in the design of effective agents against AD insults.

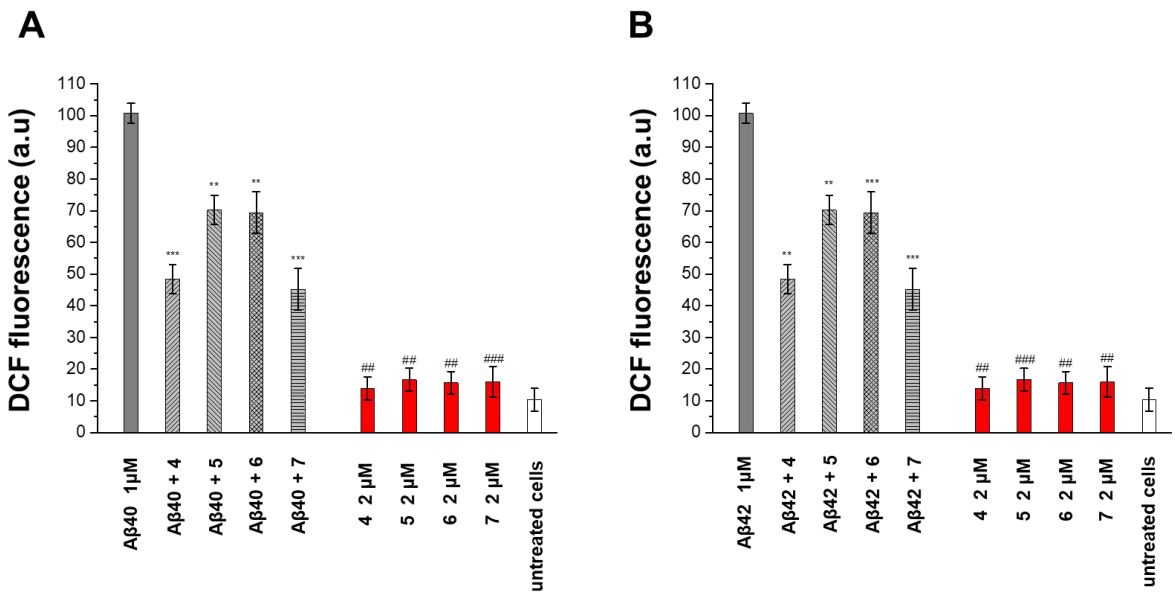

Figure 9. Effect of 2 μM of the ITSC derivatives on ROS generation induced by A*β*40 and A*β*42 (1 μM) in primary hippocampal neuronal cells after 24 h of incubation at 37 °C. ROS levels were measured by the DCF fluorescence assay (n = 3 independent experiments, each performed in six replicates). The red bars represent the effect on ROS generation of ITSCs alone. The data are presented as mean ± SEM, $^{*}p \leq 0.05$, $^{**}p \leq 0.01$, $^{***}p \leq 0.001$ compared to A*β* (1 μM) treatment and $^{\#}p < 0.01$ and $^{\#\#}p < 0.01$, $^{\#\#\#}p < 0.001$ compared to control (untreated cells).

Overall, the combined analysis of CD and ThT data indicate interaction of both A*β*40 and A*β*42 peptides with the new ITSCs, interaction which is particularly strong for derivatives **4** and **7** and leads to almost complete inhibition of formation of A*β* fibrils. In the case of A*β*40, where the random coil CD spectrum remains dominant for the duration

of the study, it appears that the majority of the interaction takes place with the monomeric (or dimeric, small oligomeric[56]) peptide. In the case of Aβ42, which is more fibrillogenic compared to Aβ40 and self-associates faster, the CD spectrum indicates the presence of a degree of β-sheet arrangement, so interaction of **4** and **7** may be taking place with a higher order Aβ42 assembly, which, nevertheless, does not further evolve into fibrils. Interaction of the ITSCs **5** and **6** with the Aβ40 and Aβ42 peptides is weaker than that of **4** and **7** allowing the eventual formation of amyloid fibrils, as shown in the ThT test, though in lower amounts and with considerable delay compared to solutions of plain peptides. The stronger activity of **4** and **7** in all cytotoxicity assays indicates a link between the inhibitory activity of Aβ aggregation and the reduction in Aβ toxicity which has been observed in the literature and merits further investigation.

This work falls into the worldwide effort to discover small-molecule based therapeutic treatment for Alzheimer's disease. A great number of organic molecules, including small peptides polyphenols, inositols, quinones and metal chelators have been reported in the literature[57] as inhibitors of Aβ aggregation. Even though the recorded cell viability values for Aβ solutions in the presence ITSCs are comparable to those observed in the presence of natural organic compounds, like olive biophenols[58], quercetin[59], rutin[60] and melatonin[48] in cell rescuing studies against Aβ toxicity, the existing experimental differences, including the cell line used, the incubation time, the concentration, protocol applied, etc., do not allow for direct comparison of our results to those in the literature. Despite the extensive *in vitro*, *in vivo* and *in silico* studies carried out to unravel the mechanism of action of small molecule aggregation inhibitors and common structural features underlying the process of inhibition, the effort has not produced a valid drug

against AD. This is mainly due to the fact that the structural identity of Aβ aggregates is not known, and Aβ aggregation process is very complex, to allow for rational design of aggregation inhibitors. In addition, promising candidates that appear, after constructing and screening libraries of compounds, are usually limited by bioavailability.[61] So the effort for novel inhibitors continues, with each study and its findings providing further insight into the mechanism of Aβ aggregation and cytotoxicity, and serving as base for design improvement. Within this framework, the present data safely establish ITSCs, and more specifically compounds **4** and **7** as highly promising Aβ inhibitors that combine a) full inhibition of Aβ aggregation as witnessed by the complete absence of Aβ typical fibrils, b) strong cytoprotective effect against Aβ insult and oxidative stress in hippocampal primary neurons and c) ease of synthesis in large amounts and in high purity. Even though our results do not allow for a clear structure-activity–relationship to be established, the thiosemicarbazone moiety emerges as an important linker for further investigation. In particular, the ITSCs **4** and **7** presented herein can be considered as privileged structures for further exploration as potential AD therapeutics and towards that goal. It is very interesting to note that in the presence of the 5-OMe isatin substitution the free indoline-2-one NH (compound **4**) was found to be of the highest antiaggregation activity, whereas the N- substituted piperidine Mannich base derivative (compound **5**) was considerably less active. Interestingly, in the case of the 5-F ITSCs (compound **6** and **7**) the opposite structure-activity relationship was observed, making the N-substituted derivative (compound **7**) the most active one and of comparable activity to that of compound **4.** This may suggest that in the case of the phenyl ITSCs a reasonable balance between the bulkiness and the electronegativity at position 5- of the isatin moiety with the

polarity of the molecule, lipophilicity and hydrogen bonding of the indole NH- group are critical for antiaggregation activity. The mechanistic investigation of the signaling pathways that they affect in wild type and AD transgenic mice (5xFAD) is currently in progress.

MATERIALS AND METHODS

All reagents used in synthesis were purchased from Sigma Aldrich and Alfa Aesar (USA), and were used without further purification. Amyloid peptides (Aβ40 and Aβ42, >95% pure) were purchased from Eurogentec (Belgium). The media/agents for the cultures of primary neuronal cells were purchased from Thermo Fisher Scientific (USA). The MTT reagent 3-(4,5-dimethylthiazol-2-yl)-2,5-diphenyltetrazolium bromide was bought from Applichem (Germany) while 2′,7′-dichlorofluorescin diacetate (DCFH-DA), thioflavin T (ThT) were bought from Sigma-Aldrich (Germany).

NMR spectra were obtained in DMSO-d_6 at 25 °C on a Bruker Avance DRX 500 MHz (^{1}H at 500.13 MHz and ^{13}C at 125.77 MHz). Tetramethylsilane (TMS) was used as the internal standard. Assignment of ^{1}H and ^{13}C chemical shifts was based on the combined analysis of a series of ^{1}H - ^{1}H and ^{1}H - ^{13}C correlation experiments recorded using standard pulse sequences from the Bruker library. The IR spectra were recorded using a Perkin-Elmer Spectrum 100 spectrometer with Universal ATR accessory (Perkin-Elmer, USA) over the range 4000 – 200 cm^{-1}. The high resolution electrospray mass spectra were recorded in the range of m/z 250 - 1400 on a TSQ 7000 Finnigan MAT (Scientific Instrument Services, USA). For the mass spectrometric studies samples were

dissolved in DMSO and the resulting solution was supplied to the electrospray capillary through a syringe pump.

The C57BL/6 mice that were used for the *in vitro* biological evaluation experiments were obtained from the breeding facilities of the Institute of Bioscience & Applications, NCSR "Demokritos". All animal procedures were carried out in compliance with the Presidential Decree 56/2013 (published in the Official Government Gazette of Greece 106 A/30-4-2013) that has transposed the EU Directive 2010/63 on the protection of animals used for scientific purposes.

Synthesis. ITSCs **4, 5** were synthesized according to previously reported procedures by reacting equimolar amounts of the commercially available substituted isatins with 4-phenyl-3-thiosemicarbazide in the presence of a catalytic amount of acetic acid. [24, 25, 36] ^{1}H and ^{13}C NMR are given in Supporting Information and are in agreement with the literature data.

General synthesis of **6, 7** [25]: A solution of the desired isatin thiosemicarbazone (2 mmol) in ethanol (20 mL) was treated with formalin (37 %, 0.20 mL, 2.5 mmol) for 15 min and then piperidine (2 mmol) was added dropwise. The reaction mixture was stirred overnight and the resulting precipitate was filtered and crystallized from ethanol.

*2-(5-methoxy-2-oxo-1-(piperidin-1-ylmethyl)indolin-3-ylidene)-N phenylhydrazinecarbothioamide (**6**)***.** This was synthesized according to the general procedure by reacting **4** with piperidine under Mannich reaction conditions. Yield 68%. IR (cm^{-1}) 1515, 1470, 1017, 3199, 1626. ^{1}H and ^{13}C NMR are given in Supporting Information. ^{1}H NMR (500 MHz, DMSO) δ 12.69 (s, 1H), 10.79 (s, 1H), 7.62 (d, J = 7.6

Hz, 2H), 7.42 – 7.38 (m, 3H), 7.27 (t, *J* = 7.8 Hz, 1H), 7.15 (d, *J* = 8.0 Hz, 1H), 6.97 (d, *J* = 8.0 Hz, 1H), 4.44 (s, 2H), 3.75 (s, 3H), 1.43 (bs, 6H), 1.30 (bs, 2H), 1.10 (bs, 2H). ^{13}C NMR (126 MHz, DMSO) δ 177.16, 162.55, 156.54, 139.16, 138.49, 132.23, 129.13, 126.94, 126.57, 120.71, 118.19, 117.75, 112.81, 107.08, 62.71, 56.42, 52.08, 26.07, 24.26; HRMS (ESI) $[M+H]^+$ calcd for $C_{22}H_{26}N_5O_2S$, 424.1802, found, 424.1796.

*2-(5-fluoro-2-oxo-1-(piperidin-1-ylmethyl)indolin-3-ylidene)-N-phenylhydrazinecarbothioamide (7)***.** This was synthesized according to the general procedure and previously reported method [25] by reacting **5** with piperidine under Mannich reaction conditions. ^{1}H and ^{13}C NMR are given in Supporting Information and are in agreement with the literature data. [25] Yield 73%.

Preparation of A*β* Stocks and Solutions. Aβ was gently dissolved without vortexing in Type 1 (Milli-Q) water to prepare a 100 μM stock solution for CD, ThT and TEM analysis and a 10 μM for cell viability and ROS measurements. Solutions of Aβ in phosphate buffer (PB, 10 mM, pH 7.33) were prepared by adding equal volumes of PB to aliquots of the aqueous solution stock to achieve the desired final concentration. For the CD, ThT and TEM studies, solutions of Aβ in phosphate buffered saline (PBS, 10 mM, pH 7.4) were prepared by adding equal volumes of PBS to aliquots of the stock to achieve final concentration of 50 μM. Proper amount of the ITSCs (stock concentration of 10 mM in DMSO) were added to the Aβ solutions to achieve a final concentration of 50 μM.

Circular Dichroism Measurements. CD spectra were recorded on a JASCO J-715 spectropolarimeter (Jasco Co., Japan), at 37 °C in the range of 190 – 260 nm with a 1 mm

path length quartz cuvette. Each spectrum was the average of three scans at a speed of 100 nm·min−1 and a resolution of 0.5 nm. CD spectra of the Aβ solutions were obtained for 30 days by CD. During this period, the Aβ solutions remained at the incubator at 37 °C without stirring. Three independent experiments were performed for each condition and in each case solutions of plain Aβ were run as control. The analysis of the CD data was performed using the OriginPro 9 program.

Thioflavin T Assay. For the ThT test 100 μL of the aged (30 days) 50 μM CD solutions of Aβ (with or without ITSCs) were diluted to half with PB (10 mM, pH 7.33) to obtain 200 μL of final solutions with theoretical Aβ concentration of 25 μM. To these solutions, a stock solution of ThT (Sigma, St. Louis, MO) in PB (10 mM, pH 7.33) was added to achieve a final concentration of ThT of 5 μM. The mixture was well agitated with pipetting and immediately thereafter, fluorescence was monitored after excitation at 440 nm (EM slit = 2.5 nm, PMT Voltage 700 V, response 0.4 s) with a HITACHI F-2500 spectrofluorometer. The analysis of the fluorescence data was performed using the OriginPro 9 program.

Transmission Electron Microscopy (TEM). For the TEM analysis, the aged (30 days) 50 μM CD solutions of Aβ42 (plain or with 100 μM ITSCs) was mixed well by pipetting. A 2 μL aliquot of this solution was placed in a carbon coated film on 200-mesh copper grids (Agar Scientific, UK) for 5 min.[62] After adsorption, the grids were washed in deionized water and negatively stained by applying a 2 μL drop of freshly prepared 1% (w/v) uranyl acetate (Sigma–Aldrich) in Milli-Q water for 5 min. Excess fluid was

blotted off and the grids were washed in deionized water and dried in air. Images were recorded using a FEI CM20 electron microscope (FEI) with a Gatan GIF 200 imaging filter (Gatan) equipped with a Peltier-cooled slow-scan charge-coupled device camera.

Cell Cultures. Hippocampal neuronal cultures were obtained from postnatal day 1 female pups of C57BL/6 mice as previously described.[63,64] Briefly, after being dissected, the hippocampus was incubated with 0.25% trypsin for 15 min at 37 °C. The hippocampi were then rinsed in 10 ml of Hibernate A containing 10% (v/v) heat-inactivated fetal bovine serum (FBS). Cultures were maintained in Neurobasal-A medium containing 2% B-27 supplement, 0.5 mM Gluta-MAX and 1% penicillin/streptomycin at 37 °C and 5% CO_2. Half of the medium was replaced twice a week. Neuronal hippocampal cells were plated at a density of approximately 2×10^4 per well in 96-well plates for MTT and ROS measurements and 5×10^5 per well in 24-well for phase-contrast microscopy. After seven days of incubation in culture well plates, the primary hippocampal neurons were harvested for the cell rescue from A*β* toxicity and ROS measurements.

Cell Rescue from A*β* Toxicity. Solutions of A*β*40 or A*β*42 (10 μM) in PBS in the presence of the ITSCs (1:1 ratio of A*β*:compounds) preincubated (3 days for all A*β*40 solutions and 1 day for all A*β*42 solutions) at 37 °C were diluted with fresh medium and added to individual wells at a final concentration of A*β* of 1 μM. Cell viability was determined by the standard MTT assay. After 24 h exposure of cells to the A*β* solutions, 100 μL of a 0.5 mg/mL stock solution of MTT in Neurobasal-A was added to each well of primary hippocampal neurons followed by a 3 h incubation at 37 °C. The medium was

removed and the cells were diluted in DMSO. The relative formazan concentration was measured by determination of the absorbance at 540 nm (Tecan well plate reader). Results were expressed as the percentage of MTT reduction, assuming that the absorbance of control (untreated) cells was 100%, and are the mean of three independent experiments with six replicate wells for each condition. In each run the effect of solutions of plain A*β* and ITSC derivatives was independently checked to serve as internal standard. Induced cell death was also qualitatively examined by phase-contrast microscopy (Axiovert 25 CFL; Carl Zeiss) using the above solutions. In each run, the effect of solutions of plain ITSCs and plain A*β*42 was independently checked to serve as internal control.

Intracellular ROS Measurements. Primary hippocampal neurons were treated with A*β* solutions following the procedure described in the *Cell Rescue from Aβ Toxicity* section. After incubation for 24 h, cells were washed with PBS and incubated with 10 μM of DCFH-DA for 30 min at 37 °C in the incubator with 5% CO_2. The fluorescence intensity (relative fluorescence unit) of DCF was determined using a Tecan fluorescence well plate reader at the excitation wavelength of 485 nm and emission wavelength of 528 nm. ROS levels are presented as arbitrary fluorescence units (AFU). Control groups consisted of cells incubated with medium only and plain A*β* or plain ITSC derivatives.

Statistical Analysis. Data in all assays are the mean of at least three independent experiments. Graphs were analyzed using GraphPad Prism 5.0 software. In hippocampal neuronal cultures the statistical significance of changes in different groups was evaluated

by one-way analysis of variance (ANOVA) and Student's t-tests, using GraphPad Prism 5.0 software. For each experiment, data are expressed as the mean ± standard error of the mean (SEM), $^{*}p \leq 0.05$, $^{**}p \leq 0.01$, $^{***}p \leq 0.001$, ns (not significant)>0.05 compared to Aβ42 (1 μM) treatment and $^{\#}p<0.01$ and $^{\#\#}p<0.01$, $^{\#\#\#}p<0.001$ compared to control (untreated cells).

ASSOCIATED CONTENT

Supporting Information

Figure S1. Structures of the Initial isatin thiosemicarbazones Library screened by CD, Synthesis, **Figure S2.** 1H NMR and 13C NMR spectra of 4, **Figure S3.** 1H NMR and 13C NMR spectra of 5, **Figure S4.** 1H NMR and 13C NMR spectra of 6, **Figure S5.** 1H NMR and 13C NMR spectra of 7, **Figure S6.** FT-IR spectra, **Figure S7.** HRMS

ABBREVIATIONS

MAO-B	Monoamine Oxidase B
Ach	Acetylcholine
DA	Dopamine
ITSCs	Isatin-3-thiosemicarbazones
HTS	High throughput screening
AD	Alzheimer disease

Aβ	β-Amyloid
CD	Circular dichroism spectropolarimetry
ThT	Thioflavin T
TEM	Transmission electron microscopy
AFU	Arbitrary fluorescence units
DCFH-DA	2′,7′-Dichlorofluorescin Diacetate
FBS	Fetal bovine serum
MTT	3-[4,5-dimethylthiazol-2-yl]-2,5-diphenyl-tetrazolium bromide

AUTHOR INFORMATION

Author affiliations

MS, BM, AK and MP - Institute of Biosciences and Applications, National Centre for Scientific Research "Demokritos", Patriarhou Grigoriou & Neapoleos 27, 15310, Athens, Greece

NB- Institute of Nanoscience and Nanotechnology, National Centre for Scientific Research "Demokritos", Patriarhou Grigoriou & Neapoleos 27, 15310, Athens, Greece

Author Contributions

MS was responsible for the study design, synthesis of ITSCs and manuscript writing; MS, BM and MP analyzed and interpreted the results and wrote the manuscript; BM

performed the CD, ThT, TEM studies under the supervision of MP; BM with AK performed the primary cell line experiments; NB prepared the TEM samples and acquired the images; MP funded and supervised the project. All authors have given approval of the final version of the manuscript.

Acknowledgments

The authors acknowledge support of this work by the projects "Target Identification and Development of Novel Approaches for Health and Environmental Applications" (MIS 5002514) which is implemented under the Action for the Strategic Development on the Research and Technological Sectors, and "A Greek Research Infrastructure for Visualizing and Monitoring Fundamental Biological Processes (BioImaging-GR)" (MIS 5002755) which is implemented under the Action "Reinforcement of the Research and Innovation Infrastructure". Both projects are funded by the Operational Programme "Competitiveness, Entrepreneurship and Innovation" (NSRF 2014-2020) and co-financed by Greece and the European Union (European Regional Development Fund)." M. Pelecanou acknowledges financial support by HYGEIA Hospital, Athens, Greece and B. Mavroidi gratefully acknowledges financial support by Stavros Niarchos Foundation (SNF) through implementation of the program of Industrial Fellowships at NCSR "Demokritos". The graphical abstract was created by A.K. with “biorender.com”.

Conflicts of interest

The authors declare no conflict of interest about this article.

REFERENCES

1. Erdmann, O. L. Untersuchungen über den Indigo. *J. Prakt. Chem.* **1840**, *19*, 321–362.

2. Laurent, A. Recherches sur l'indigo. *Ann. Chim. Phys*. **1840**, *3*, 393–434.

3. Guo, Y.; Chen, F. TLC-UV-spectrophotometric and TLC-scanning determination of isatin in leaf of Isatis. *Chin. Trad. Herb. Drugs*. **1986**, *17*, 8-11.

4. Bergman, J.; Lindström, J. O.; Tilstam, U. The structure and properties of some indolic constituents in Couroupita guianensis aubl. *Tetrahedron.* **1985**, *41*, 2879-2881.

5. Wei, L.; Wang, Q.; Liu, X. Application of thin-layer chromatography in quality control of Chinese medicinal preparations. II. Qualitative analysis of some Chinese medicinal preparations of Chansu. *Yaowu Fenxi Zazhi*. **1982**, *2*, 288-291.

6. Medvedev, A.; Buneeva, O.; Glover, V. Biological targets for isatin and its analogues: implications for therapy. *Biologics*. **2007**, *1*, 151-162

7. Glover V.; Halket JM.; Watkins PJ.; Clow A.; Goodwin BL.; Sandler M., Isatin: identity with the purified endogenous monoamine oxidase inhibitor tribulin. *J Neurochem,* **1988**, *51*, 656-9.

8. Medvedev A.; Buneeva O.; Gnedenko O.; Ershov P.; Ivanov A. Isatin, an endogenous nonpeptide biofactor: A review of its molecular targets, mechanisms of actions, and their biomedical implications. *Biofactors,* **2018**, *44*, 95-108.

9. Binda, C.; Li, M.; Hubalek, F.; Restelli, N.; Edmondson, D.E.; Mattevi, A. Insights Into the Mode of Inhibition of Human Mitochondrial Monoamine Oxidase B from High-Resolution Crystal Structures, *Proc. Natl. Acad. Sci. USA,* **2003**, *100*, 9750

10. Hamaue, N.; Yamazaki, N.; Minami, M.; Endo, T.; Hirafuji, M.; Monma, Y.; Togashi, H.; Saito, H.; Parvez, S. H.; (1999) Effects of isatin, an endogenous MAO inhibitor, on acetylcholine and dopamine levels in the rat striatum. *Biog Amines*, **1999**, *15*, 367–377

11. Pakravan, P.; Kashanian, S.; Khodaei, M. M.; Harding, F. J. Biochemical and pharmacological characterization of isatin and its derivatives: from structure to activity. *Pharmacol. Rep*. **2013**, *65*, 313-335.

12. Khan, F. A.; Maalik, A. Advances in Pharmacology of Isatin and its Derivatives: A Review. *Trop. J. Pharm. Res*. **2015**, *10*, 1937-1942.

13. Grewal, A.S. Isatin derivatives with several biological activities. *Int. J. Pharm. Res*. **2014**, *6*, 1-7.

14. Mok, N. Y.; Chadwick, J.; Kellett, K. A. B.; Hooper, N. M.; Johnson, A. P.; Fishwick, C. W. G. Discovery of novel non-peptide inhibitors of BACE-1 using virtual high-throughput screening. *Bioorg. Med. Chem. Lett*. **2009**, *23*, 6770-6774.

15. McKoy, A. F.; Chen, J.; Schupbach, T.; Hecht, M. H. A novel inhibitor of amyloid peptide aggregation: from high throughput screening to efficacy in an animal model of alzheimer disease. *J. Biol. Chem.* **2012**, *46*, 38992–39000.

16. Purgatorio, R.; De Candia, M.; De Palma, A.; De Santis, F.; Pisani, L.; Campagna, F.; Cellamare, S.; Altomare, C. D.; Catto, M. Insights into structure-activity relationships of 3-arylhydrazonoindolin-2-one derivatives for their multitarget activity on beta amyloid aggregation and neurotoxicity. *Molecules*. **2018**, *23*, 1-23.

17. Campagna, F.; Catto, M.; Purgatorio, R.; Altomare, C. D.; Carotti, A.; De Stradis, A.; Palazzo, G. Synthesis and biophysical evaluation of arylhydrazono-1H-2-indolinones as β-amyloid aggregation inhibitors. *Eur. J. Med. Chem.* **2011**, *1*, 275-284.

18. Catto, M.; Aliano, R.; Carotti, A.; Cellamare, S.; Palluotto, F.; Purgatorio, R.; De Stradis, A.; Campagna, F. Design, synthesis and biological evaluation of indane-2-arylhydrazinylmethylene-1,3-diones and indol-2-aryldiazenylmethylene-3-ones as beta-amyloid aggregation inhibitors. *Eur. J. Med. Chem*. **2010**, *45*, 1359–1366.

19. Catto, M.; Arnesano, F.; Palazzo, G.; De Stradis, A.; Calò, V.; Losacco, M.; Purgatorio, R.; Campagna, F. Investigation on the Influence of (Z)-3-(2-(3-Chlorophenyl)hydrazono)-5,6-dihydroxyindolin-2-one (PT2) on amyloid(1-40) Aggregation and Toxicity. *Arch. Biochem. Biophys.* **2014**, *560*, 73–82.

20. Pisani, L.; De Palma, A.; Giangregorio, N.; Miniero, D.V.; Pesce, P.; Nicolotti, O.; Campagna, F.; Altomare, C.D.; Catto, M. Mannich base approach to 5-methoxyisatin 3-(4-isopropylphenyl)hydrazone: A water-soluble prodrug for a multitarget inhibition of cholinesterases, beta-amyloid fibrillization and oligomer-induced cytotoxicity. *Eur. J. Pharm. Sci.* **2017**, *109*, 381–388.

21. Cohen T.; Frydman-Marom A.; Rechter M.; Gazit E. Inhibition of amyloid fibril formation and cytotoxicity by hydroxyindole derivatives. *Biochemistry*. **2006**, *45*, 4727-4735.

22. Convertino, M.; Pellarin, R.; Catto, M.; Carotti, A.; Caflisch, A. 9,10-Anthraquinone hinders β-aggregation: How does a small molecule interfere with Aβ-peptide amyloid fibrillation? *Protein Sci*. **2009**, *18*, 792-800.

23. Cellamare, S.; Stefanachi, A.; Stolfa, D.A.; Basile, T.; Catto, M.; Campagna, F.; Sotelo, E.; Acquafredda, P.; Carotti, A. Design, Synthesis, and Biological Evaluation of Glycine-based Molecular Tongs as Inhibitors of Abeta1-40 Aggregation in Vitro. *Bioorg. Med. Chem.* **2008**, *16*, 4810–4822.

24. García Fernández-Luna V.; Mallinson, D.; Alexiou, P.; Khadra, I.; Mullen, A. B.; Pelecanou, M.; Sagnou, M.; Lamprou, D. A Isatin thiosemicarbazones promote honeycomb structure formation in spin-coated polymer films: concentration effect and release studies, *RSC Adv*. **2017**, *7*, 12945-12952.

25. Mallinson, D.; Alexiou, P.; Mullen, A. B.; Pelecanou, M.; Sagnou, M.; Lamprou, D. A. Isatin thiosemicarbazone-blended polymer films for biomedical applications: Surface morphology, characterization and preliminary biological assessment. *RSC Adv*. **2016**, *6*, 24939-24945.

26. Sagnou, M.; Mavroidi, B.; Shegani, A.; Paravatou-Petsotas, M.; Raptopoulou, C.; Psycharis, V.; Pirmettis, I.; Papadopoulos, M. S.; Pelecanou, M. Remarkable brain penetration of cyclopentadienyl $m(co)_3^+$ (m = ^{99m}tc, re) derivatives of benzothiazole and benzimidazole paves the way for their application as diagnostic, with single-photon-

emission computed tomography (SPECT), and therapeutic agents for Alzheimer's disease. *J. Med. Chem.* **2019**, *5*, 2638-2650.

27. Matis, I.; Delivoria, D. C.; Mavroidi, B.; Papaevgeniou, N.;Panoutsou, S.; Bellou, S.; Papavasileiou, K. D.; Linardaki, Z. I.;Stavropoulou, A. V.; Vekrellis, K.; Boukos, N.; Kolisis, F. N.; Gonos,E. S.; Margarity, M.; Papadopoulos, M. G.; Efthimiopoulos, S.;Pelecanou, M.; Chondrogianni, N.; Skretas, G. An integrated bacterialsystem for the discovery of chemical rescuers of disease-associatedprotein misfolding. *Nat. Biomed. Eng.* **2017**,*1*, 838−852.

28. Donnelly, P.; Caragounis, A.; Du, T.; Laughton, K.; Volitakis, I.; Cherny, R.;. Sharples, R.; Hill, A.; Li, Q.; Masters, C.L.; Barnham, K.; White, A. Selective intracellular release of copper and zinc ions from bis(thiosemicarbazonato) complexes reduces levels of alzheimer disease amyloid-peptide. *J. Biol. Chem.* **2008**, *283,* 4568-4577.

29. Haribabu, J.; Ranade, D. S.; Bhuvanesh, N. S. P.; Kulkarni, P. P.; Karvembu, R. Ru(II)-p-cymene Thiosemicarbazone Complexes as Inhibitors of Amyloid b (Ab) Peptide Aggregation and Ab-Induced Cytotoxicity. *ChemistrySelect.* **2017,** *2*, 11638 –11644

30. Ranade, D. S.; Bapat, A. M.; Ramteke, S. N.; Joshi, B. N.; Roussel, P.; Deschamps T. A.; Kulkarni, P. P. Thiosemicarbazone modification of 3-acetyl coumarin inhibits Aβ peptide aggregation and protect against Aβ-induced cytotoxicity. *Eur. J. Med Chem.* **2016**, *121*, 803-809.

31. Ranade, D. S.; Shravage, B. V.; Kumbhar, A. A.; Sonawane, U. B.; Jani, V. P.; Joshi, R. R.; Kulkarni, P. P. Thiosemicarbazone Moiety Assist in Interaction of Planar Aromatic

Molecules with Amyloid Beta Peptide and Acetylcholinesterase. *ChemistrySelect.* **2017**, *13*, 3911-3916.

32. Park, D.H.; Venkatesan, J.; Kim, S.K.; Ramkumar, V.; Parthiban, P. Antioxidant properties of Mannich bases, *Bioorg. Med. Chem. Lett.*, **2012**, *22*, 6362-6367.

33. Fang, L.; Gou, S.; Liu, X.; Cao, F.; Cheng, L. Design, synthesis and anti-Alzheimer properties of dimethylaminomethyl-substituted curcumin derivatives. *Bioorg. Med. Chem. Lett*. **2014**, *24*, 40-43.

34. Kontogiorgis, C. A.; Hadjipavlou-Litina, D. J. Synthesis and antiinflammatory activity of coumarin derivatives. *J. Med. Chem*. **2005**, *48*, 6400-6408.

35. Roman, G. Mannich bases in medicinal chemistry and drug design. *Eur. J. Med. Chem.* **2015**, *89*, 743-816.

36. Hall, M. D.; Salam, N. K.; Hellawell, J. L.; Fales, H. M.; Kensler, C. B.; Ludwig, G. A.; Szakacs, G.; Hibbs, D. E.; Gottesman, M. M. Synthesis, activity and pharmacophore development for isatin-β-thiosemicarbazones with selective activity towards multidrug resistant cells. *J. Med. Chem.* **2009**, *10*, 3191–3204.

37. Pandeya, S. N.; Sriram, D.; Nath, G.; DeClercq, E. Synthesis, antibacterial, antifungal and anti-HIV activities of Schiff and Mannich bases derived from isatin derivatives and N-[4-(49-chlorophenyl)thiazol-2-yl] thiosemicarbazide. *Eur. J. Pharm. Sci.* **1999**, *9*, 25–31.

38. Lim, K. H. Characterizations of distinct amyloidogenic conformations of the Aβ (1–40) and (1–42) peptides. *Biochem. Biophys. Res. Commun.* **2007**, *353*, 443–449.

39. Barrow CJ.; Yasuda, A.; Kenny, PT.; Zagorski, MG. Solution Conformations and Aggregational Properties of Synthetic Amyloid Beta-Peptides of Alzheimers-Disease - Analysis of Circular-Dichroism Spectra. *J Mol Biol*, **1992,** *225*, 1075-1093**.**

40. LeVine, H. Thioflavine T interaction with synthetic Alzheimer's disease beta-amyloid peptides: detection of amyloid aggregation in solution. *Protein Sci.* **1993**, *3*, 404–410.

41. Vandersteen, A.; Masman, M. F.; De Baets, G.; Jonckheere, W.; Van der Werf, K.; Marrink, S. J.; Rozenski, J.; Benilova, I.; De Strooper, B.; Subramaniam, V.; Schymkowitz, J.; Rousseau, F.; Broersen, K. Molecular plasticity regulates oligomerization and cytotoxicity of the multipeptide-length amyloid-beta peptide pool. *J. Biol. Chem.* **2012,** *44*, 36732-36743.

42. Francioso, A.; Punzi, P.; Boffi, A.; Lori, C.; Martire, S.; Giordano, C.; D'Erme, M.; Mosca, L. beta-sheet interfering molecules acting against beta-amyloid aggregation and fibrillogenesis. *Bioorg. Med. Chem.* **2015**, *8*, 1671-1683.

43. Guerrero-Muñoz, M. J.; Castillo-Carranza, D. L.; Kayed, R. Therapeutic approaches against common structural features of toxic oligomers shared by multiple amyloidogenic proteins. *Biochem. Pharmacol.* **2014**, *4*, 468-478.

44. Mu, Y.; Gage, F. H. Adult hippocampal neurogenesis and its role in Alzheimer's disease. *Mol. Neurodegener.* **2011**, *6*, 1-9.

45. Bitan, G.; Kirkitadze, M. D.; Lomakin, A.; Vollers, S. S.; Benedek, G. B.; Teplow, T. B. Amyloid beta -protein (Abeta) assembly: Abeta 40 and Abeta 42 oligomerize through distinct pathways. *Proc. Natl. Acad. Sci. USA.* **2003**, *1*, 330-335.

46. Kai, T.; Zhang, L.; Wang, X.; Jing, A.; Zhao, B.; Yu, X.; Zheng, J.; Zhou, F. Tabersonine inhibits amyloid fibril formation and cytotoxicity of Aβ(1-42). *ACS Chem. Neurosci.* **2015** *6*, 879-888.

47. Chyan, Y. J.; Poeggeler, B.; Omar R. A.; Chain, D. G.; Frangione, B.; Ghiso, J.; Pappolla, M. A. Potent neuroprotective properties against the Alzheimer beta-amyloid by

an endogenous melatonin-related indole structure, indole-3-propionic acid. *J. Biol. Chem.* **1999**, *31*, 21937-21942.

48. Pappolla, M. A.; Sos, M.; Omar, R. A.; Bick, R. J.; Hickson-Bick, D. L.; Reiter, R. J.; Efthimiopoulos, S.; Robakis, N. K. Melatonin prevents death of neuroblastoma cells exposed to the Alzheimer amyloid peptide. *J. Neurosci.* **1997**, *5*, 1683-1690.

49. Alobuia W.M.; Xia W.; Vohra, B.P.S. Axon degeneration is key component of neuronal death in amyloid - β toxicity, *Neurochem Int.* **2013,** *63*, 782–789.

50. Cheignon, C.; Tomas, M.; Bonnefont-Rousselot, D.; Faller, P.; Hureau, C.; Collin, F. Oxidative stress and the amyloid beta peptide in Alzheimer's disease. *Redox Biol.* **2018**, *14*, 450–464.

51. Butterfield, D. A.; Lauderback, C. M. Lipid peroxidation and protein oxidation in Alzheimer's disease brain: potential causes and consequences involving amyloid beta-peptide-associated free radical oxidative stress. *Free Radic. Biol. Med.* **2002**, *11*, 1050–1060.

52. Guglielmotto, M..; Giliberto, L.; Tamagno, E.; Tabaton, M. Oxidative stress mediates the pathogenic effect of different Alzheimer's disease risk factors. *Front. Aging Neurosci.* **2010**, *2*, 1-8.

53. Wang, H.; Joseph, J. A. Quantifying cellular oxidative stress by dichlorofluorescein assay using microplate reader. *Free Radic. Biol. Med.* **1999**, *5-6*, 612-616.

54. Ahmad, F.; Singh, K.; Das, D.; Gowaikar, R.; Shaw, E.; Ramachandran, A.; Valli Rupanagudi, K.; Peera Kommaddi, R.; Bennett, D.A; Ravindranath, V. *Antioxid. Redox Signal.* **2017**, *27*, 1269-1280.

55. Carrillo-Mora, P.; R. Luna; Colin-Barenque, L. Amyloid Beta: Multiple Mechanisms of Toxicity and Only Some Protective Effects? *Oxid Med Cell Longev.* **2014***; 795375,* 15.

56. Tsigelny, I.F.; Sharikov, Y.; Kouznetsova, V. L.; Greenberg, J. P.; Wrasidlo, W.; Gonzalez, T.; Desplats, P.; Michael, S. E.; Trejo-Morales, M.; Overk, C. R.; & Masliah, E. Structural diversity of Alzheimer's disease amyloid-beta dimers and their role in oligomerization and fibril formation. *J Alzheimers Dis,* **2014.** *39*, 583-600**.**

57. Jokar, S.; Khazaei, S.; Behnammanesh, H.; Shamloo, A.; Erfani, M.; Beiki, D.; Bavi, O. Recent advances in the design and applications of amyloid-β peptide aggregation inhibitors for Alzheimer's disease therapy. *Biophys. Rev.* **2019,** *11,* 901–925

58. Omar, S. H.; Scott, C. J.; Hamlin, A. S.; Obied, H. K. Olive Biophenols Reduces Alzheimer's Pathology in SH-SY5Y Cells and APPswe Mice. *Int. J. Mol. Sci.* **2018**, 1, 1-23.

59. Ansari, M. A.; Abdul, H. M.; Joshi, G.; Opii, W. O.; Butterfield, D. A. Protective effect of quercetin in primary neurons against Aβ (1–42): relevance to Alzheimer's disease. *J. Nutr. Biochem.* **2009**, *4*, 269–275.

60. Enogieru, A. B.; Haylett, W.; Hiss, D. C.; Bardien, S.; Ekpo, O. E. Rutin as a Potent Antioxidant: Implications for Neurodegenerative Disorders. *Oxid. Med. Cell Longev.* **2018**, 1-17.

61. Brahmachari, S.; Paul, A.; Segal, D.; Gazit, E. Inhibition of amyloid oligomerization into different supramolecular architectures by small molecules: mechanistic insights and design rules. *Fut Med Chem,* **2017**. *9*, 797-810.

62. Broersen, K.; Jonckheere, W.; Rozenski, J.; Vandersteen, A.; Pauwels, K.; Pastore, A.; Rousseau, F.; Schymkowitz, J. A standardized and biocompatible preparation of

aggregate-free amyloid beta peptide for biophysical and biological studies of Alzheimer's disease. *Protein Eng. Des. Sel.* **2011**, *9*, 743-750

63. Brewer, G. J.; Torricelli, J. R. Isolation and culture of adult neurons and neurospheres. *Nat. Protoc.* **2007**, *6*, 1490-1498.

64. Kaminari, A.; Giannakas, N.; Tzinia, A.; Tsilibary, E. C. Overexpression of matrix metalloproteinase-9 (MMP-9) rescues insulin-mediated impairment in the 5XFAD model of Alzheimer's disease. *Sci. Rep.* **2017**, *1*, 1-12.

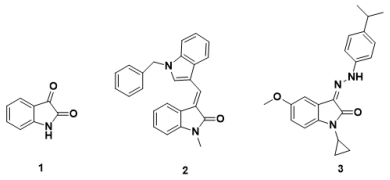

Figure 1. Chemical structures of isatin (1) and other active indole derivatives (2, 3) in the literature.

338x190mm (96 x 96 DPI)

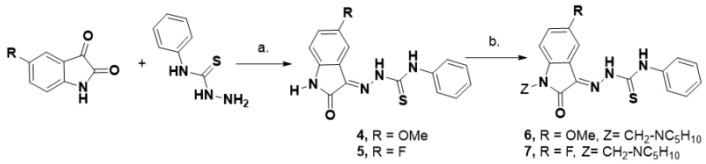

Scheme 1. Synthetic route of the ITSC derivativesa

338x190mm (96 x 96 DPI)

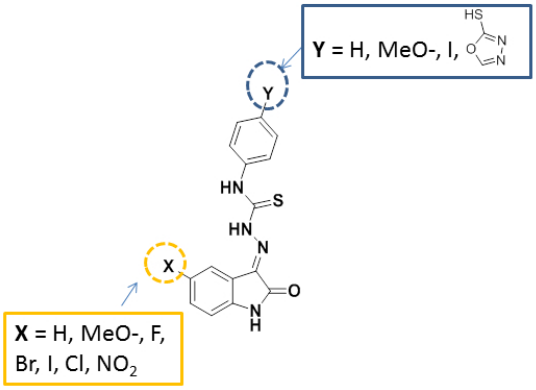

Figure 2. The design of the initial library of ITSCs

254x190mm (96 x 96 DPI)

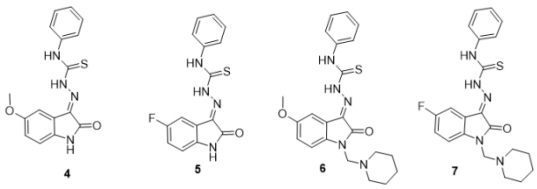

Figure 3. Chemical structures of the ITSC derivatives 4 - 7 of this work.

338x190mm (96 x 96 DPI)

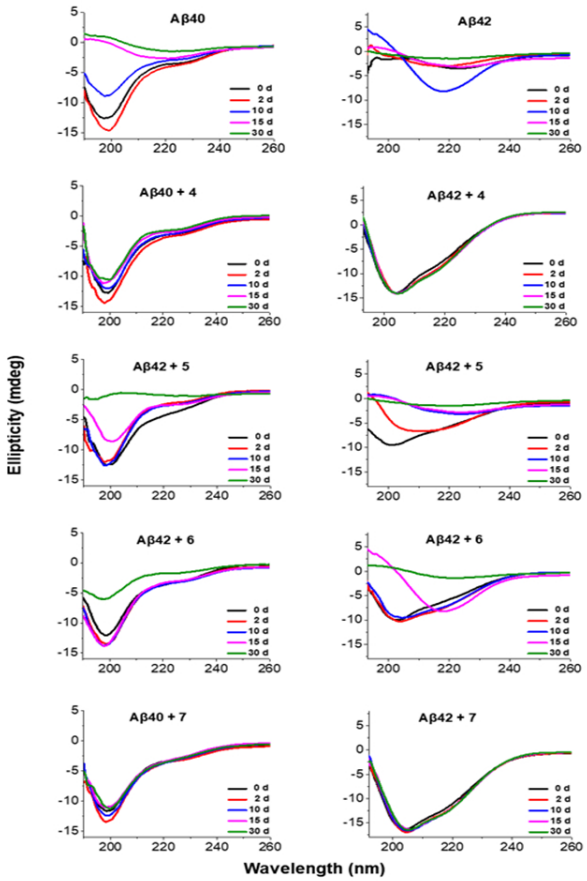

Figure 4. CD spectra of plain solutions of Aβ40 and Aβ42 (50 μM) as well as in the presence of the ITSC derivatives (Aβ:ITSCs ratio 1:1). Spectra were recorded for a period of 30 days at 37 °C. Representative spectra from n = 3 independent experiments are presented.

190x338mm (96 x 96 DPI)

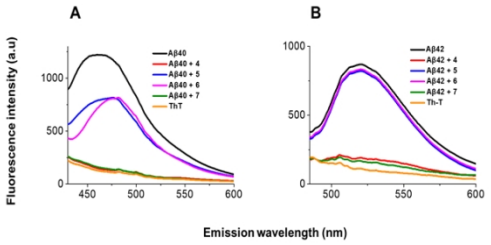

Figure 5. Aβ aggregation assay using fluorescence emission of ThT upon binding to aggregated Aβ (25 μM, 30 d). A lower intensity than that of plain Aβ solutions ThT (black line) indicates lower concentration of Aβ fibrils. (A) Aβ40 solutions in the absence and presence of ITSCs and (B) Aβ42 solutions in the absence and presence of ITSCs. Fluorescence was monitored after excitation at λ = 440 nm. Representative spectra from n = 3 independent experiments are presented

338x190mm (96 x 96 DPI)

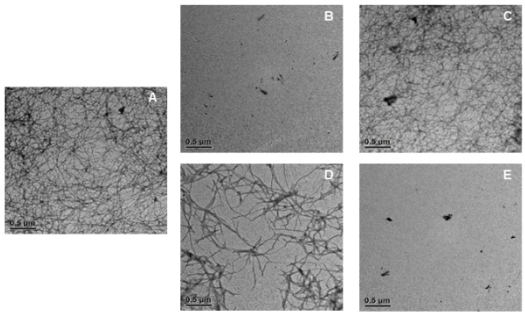

Figure 6. TEM images of the aged Aβ42 solutions (30 d, 50 μM) used for the CD evaluation in the absence (A) and the presence of compounds 4 and 7 (50 μM, B and E), where complete lack of fibrils was observed and 5 and 6 (50 μM, C and D) where fibril formation has taken place. The scale bars correspond to 0.5 μm. Representative images from n = 2 independent experiments are presented.

338x190mm (96 x 96 DPI)

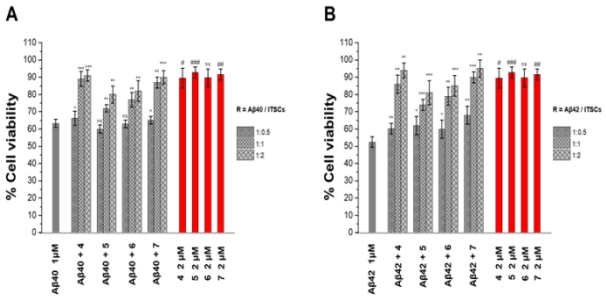

Figure 7. Effects of the ITSC derivatives (0.5, 1 and 2 μM) on the cytotoxicity of Aβ40 (A) or Aβ42 (B) (1 μM) in primary hippocampal neuronal cells after 24 h of incubation at 37 °C, as determined using the MTT assay (n = 3 independent experiments, each one performed in six replicates). The red bars represent the effect on the cell viability of ITSCs alone. The data are presented as mean ± SEM, *p≤0.05, **p≤0.01, ***p≤0.001, ns (not significant)>0.05 compared to Aβ (1 μM) treatment and #p<0.01 and ##p<0.01, ###p<0.001 compared to control (untreated cells).

338x190mm (96 x 96 DPI)

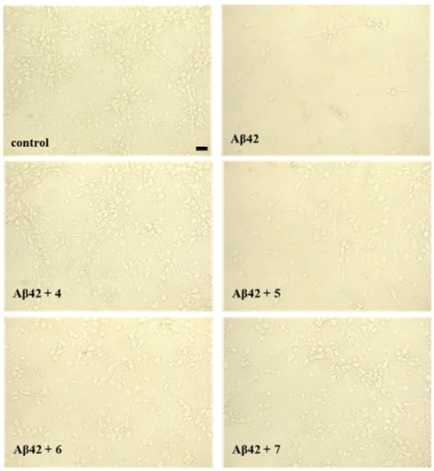

Figure 8. Phase-contrast microscopy images of primary hippocampal neuronal cells exposed for 24 h at 37 °C to pre-incubated Aβ42 solutions (1 μM) in the absence or in the presence of ITSC derivatives (2 μM). The scale bar corresponds to 50 μm. Representative images from n = 2 independent experiments are presented.

338x190mm (96 x 96 DPI)

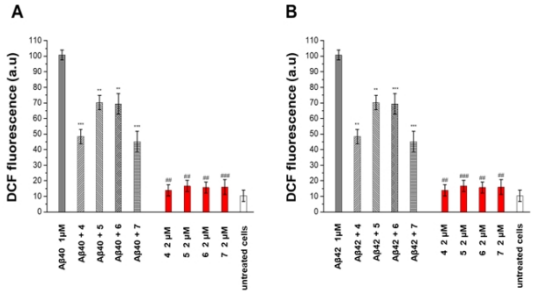

Figure 9. Effect of 2 μM of the ITSC derivatives on ROS generation induced by Aβ40 and Aβ42 (1 μM) in primary hippocampal neuronal cells after 24 h of incubation at 37 °C. ROS levels were measured by the DCF fluorescence assay (n = 3 independent experiments, each performed in six replicates). The red bars represent the effect on ROS generation of ITSCs alone. The data are presented as mean ± SEM, *p≤0.05, **p≤0.01, ***p≤0.001 compared to Aβ (1 μM) treatment and #p<0.01 and ##p<0.01, ###p<0.001 compared to control (untreated cells).

338x190mm (96 x 96 DPI)

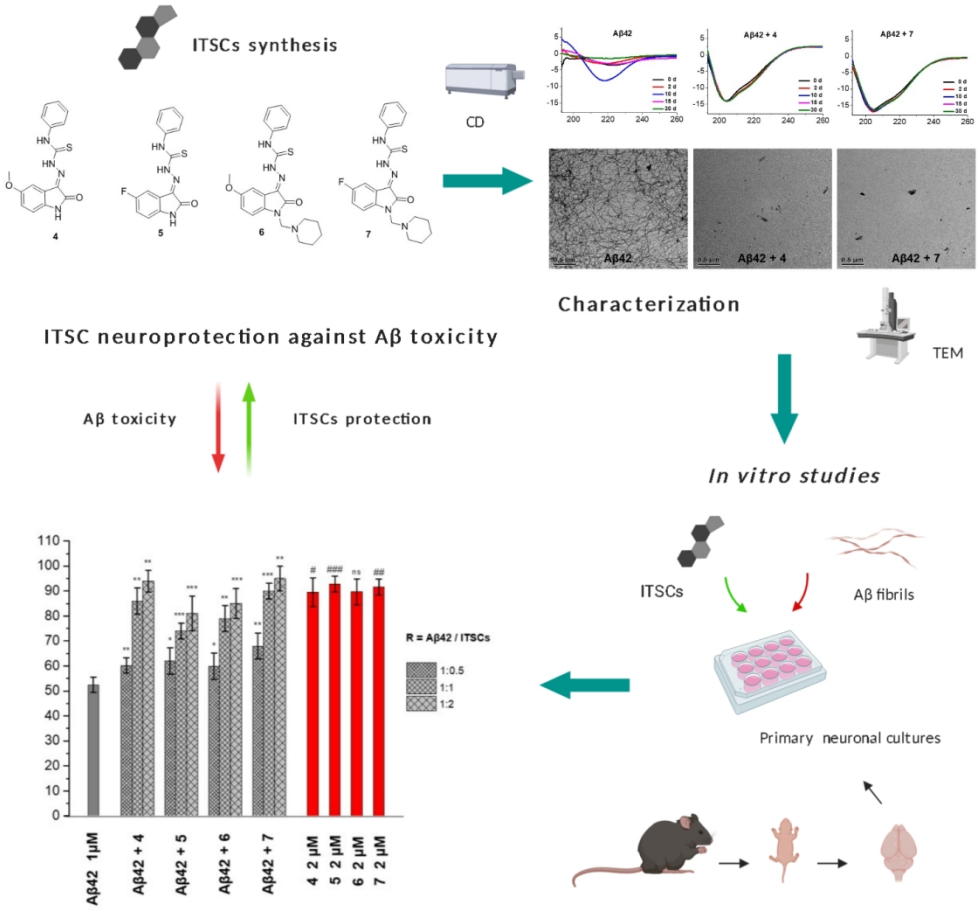
ITSCs synthesis
CD
Characterization
TEM
ITSC neuroprotection against Aβ toxicity
Aβ toxicity
ITSCs protection
In vitro studies
ITSCs
Aβ fibrils
Primary neuronal cultures
R = Aβ42 / ITSCs
1:0.5
1:1
1:2
Aβ42 1μM
Aβ42 + 4
Aβ42 + 5
Aβ42 + 6
Aβ42 + 7
4 2 μM
5 2 μM
6 2 μM
7 2 μM